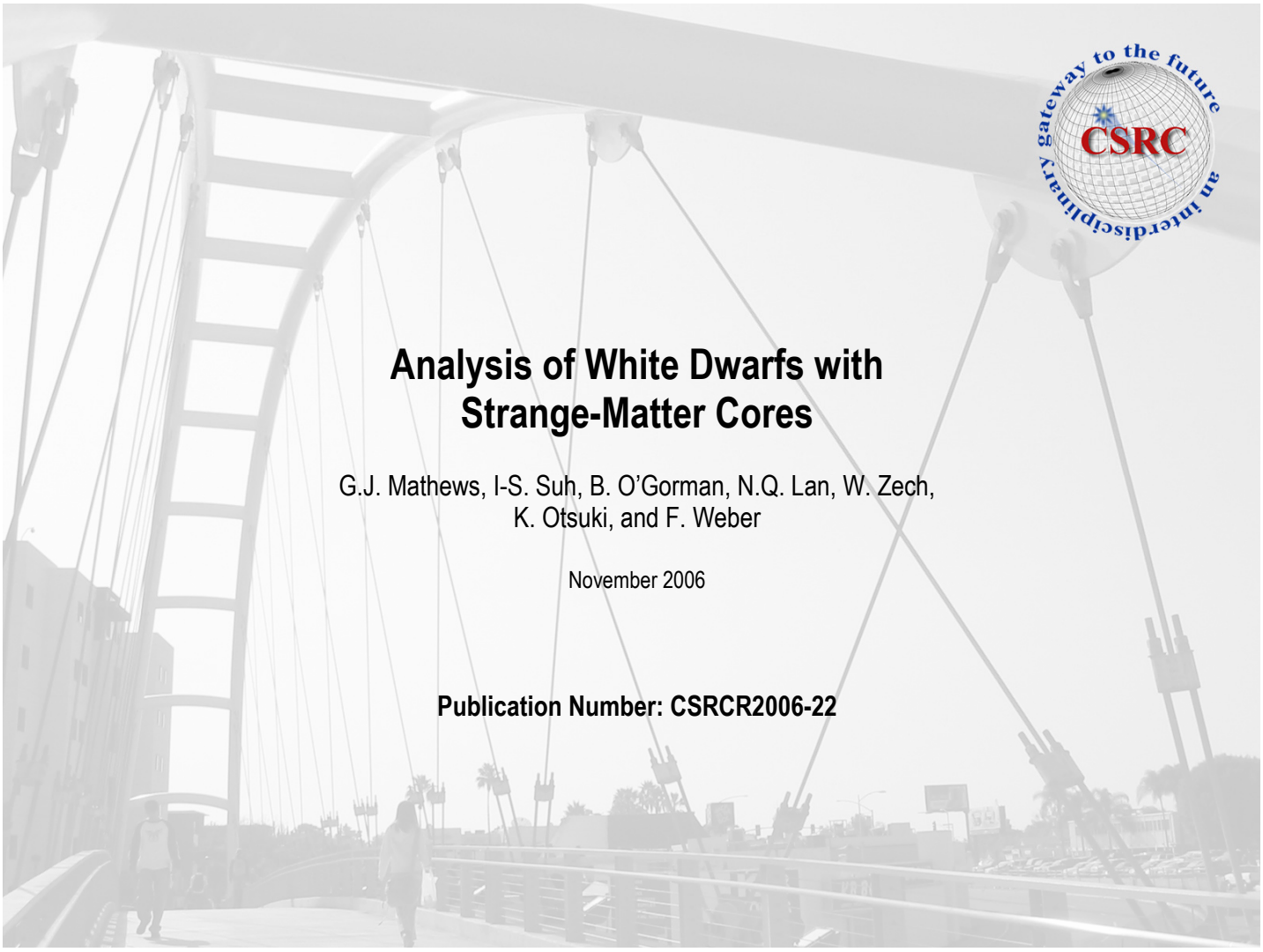

Analysis of White Dwarfs with Strange-Matter Cores

G.J. Mathews, I-S. Suh, B. O'Gorman, N.Q. Lan, W. Zech,
K. Otsuki, and F. Weber

November 2006

Publication Number: CSRCR2006-22

Computational Science & Engineering Faculty and Students Research Articles

Database Powered by the Computational Science Research Center Computing Group

COMPUTATIONAL SCIENCE & ENGINEERING

SAN DIEGO STATE UNIVERSITY

Computational Science Research Center
College of Sciences
5500 Campanile Drive
San Diego, CA 92182-1245
(619) 594-3430

Analysis of White Dwarfs with Strange-Matter Cores

G. J. Mathews[1], I.-S. Suh[2], B. O'Gorman[1], N. Q. Lan[1], W. Zech[1], K. Otsuki[3], F. Weber[4]
[1] *Center for Astrophysics, Department of Physics, University of Notre Dame, Notre Dame, IN 46556*
[2] *Center for Research Computing, University of Notre Dame, Notre Dame, IN 46556*
[3] *University of Chicago, Chicago,IL 60637*
[4] *Department of Physics, San Diego State University San Diego, CA 92182*
(Dated: April 19, 2006)

We summarize masses and radii for a number of white dwarfs as deduced from a combination of proper motion studies, *Hipparcos* parallax distances, effective temperatures, and binary or spectroscopic masses. A puzzling feature of these data, however, is that some stars appear to have radii which are significantly smaller than that expected for a standard electron-degenerate white-dwarf equations of state. We construct a projection of white-dwarf radii for fixed effective mass and conclude that there is at least marginal evidence for bimodality in the radius distribution for white dwarfs. We argue that if such compact white dwarfs exist it is unlikely that they contain an iron core. We propose an alternative of strange-quark matter within the white-dwarf core. We also discuss the impact of the so-called color-flavor locked (CFL) state in strange-matter core associated with color superconductivity. We show that the data exhibit several features consistent with the expected mass-radius relation of strange dwarfs. We identify eight nearby white dwarfs which are possible candidates for strange matter cores and suggest observational tests of this hypothesis.

I. INTRODUCTION

The possible existence of strange-matter stars has been speculated upon for some time. Most of the work concerning their nature and origin has focused on neutron stars (cf. [11]). Indeed, there have been many suggestions of possible observational evidence of neutron stars which are too compact or have cooled too rapidly to be comprised of normal nuclear matter. Although the first reports [7, 29] of strange-matter stars seem ruled out, other good candidates remain [3, 22, 28, 34, 41].

In this paper we are concerned with the possible existence of white dwarfs with strange-matter cores as has been proposed by Glendenning et al. [9, 10] who coined the term *strange dwarfs*. Although, the central density and temperature of white dwarfs are too low to allow a spontaneous transition to strangelets (such as may occur in hot proto-neutron stars [1]), strange-matter white dwarfs could gradually form [9, 10] during the progenitor main-sequence by the accretion of a strange-matter nugget. Such nuggets could exist either as a relic of the early universe or as an ejected fragment from the merger/coalescence of strange-matter neutron stars. Once captured by a star, strange-matter nuggets would gravitationally settle to the center and begin to convert normal matter to strange matter. This would eventually lead to the formation of an extended strange-quark-matter core in the white dwarf remnant.

However unlikely this paradigm may seem, we nevertheless think it worthwhile to examine the evidence for the possible existence of a population of such peculiar white dwarfs. The most distinguishing characteristic of the existence of strange dwarfs is that they must have a smaller radius. This unavoidable consequence simply follows from the fact that strange-matter has more degrees of freedom and can therefore be more compact than ordinary electron-degenerate matter. In this paper we expand on a previous study [33] aimed at identifying nearby candidate white dwarfs with strange matter cores. We review the evidence for two populations of white dwarfs, one of which is more compact. We present an updated list of nearby stars with best determined masses and radii which are consistent with the existence of a strange-matter core. We propose some observational tests of this hypothesis.

A. Data

The quality and quantity of observational data on the white-dwarf mass-radius relation has been improved in recent years due to the accumulation of expanded proper motion surveys (e.g. [5]) and the availability of *Hipparcos* parallax distances for a number of white dwarfs. For example, Provencal et al. [24] used *Hipparcos* data to deduce luminosity radii for 10 white dwarfs in visual binaries or common proper-motion systems as well as 11 field white dwarfs. Complementary *HST* observations have also been made, for example to better determine the spectroscopy for *Procyon B* [25] and the pulsation of *G226-29* [19]. *Procyon B* at first appeared as a compact star in [24]. In [25],

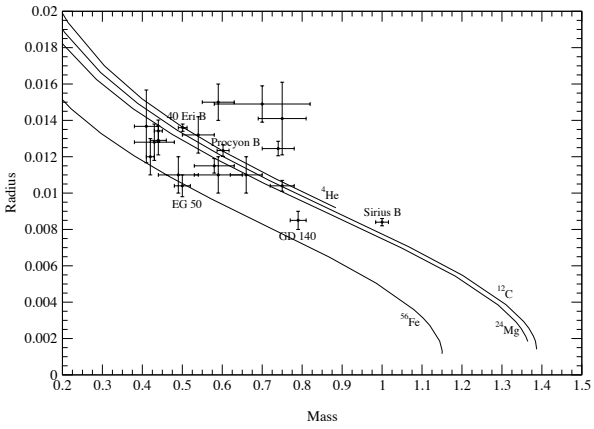

FIG. 1: The mass M and radius R for the 22 white dwarfs [24, 25]. The solid lines denote the Hamada & Salpeter model for normal white dwarfs with the indicated composition.

however, this star is now confirmed to lie on the normal white-dwarf mass-radius relation. This fact was missed in [33]. Nevertheless, several other stars in this sample still appear to be compact.

A summary of our adopted masses and radii for 22 nearby white dwarfs [from [24, 25]] is presented in Table 1. When more than one method was used to determine masses, the astrometric mass was taken to be better than the spectroscopic mass [except for *Stein 2051B* for which we adopt the spectroscopic mass as in [25]]. Lowest priority was given to gravitational mass estimates as the inferred masses and radii assume a model for the white dwarf structure. (Indeed, there is no evidence of 2 populations in the survey of [5] which we attribute to this systematic effect). All radii are based upon the Stefan-Boltzmann radius inferred from the observed luminosity and *Hipparcos* distances or the gravitational redshift. We note that since the *Hipparcos* mission, critical assessments have been made [32] of the of the data quality, and although some problems have been identified, the catalogue as published remains generally reliable within the quoted accuracies and can continue to be adopted here. We also note that radii quoted in table 5 of [24] for two of the stars (L481-60 and G154-B5B) are inconsistent with the measured gravitational redshift given in table 4 of that paper. The radii listed in table 1 have been corrected to be consistent with the observed gravitational redshift.

These data are compared with standard [13] mass-radius relations for He, C/O, and Mg white dwarfs in Figure 1. It is readily apparent that some of the best determined radii, e.g. *EG 50* and *GD 140*, seem significantly more compact than that deduced from a normal electron-degenerate equation of state. *EG 50* has a well determined mass as it is a member of a visual binary. The mass of the field white dwarf *GD 140* is also well determined. It has been well studied spectroscopically as its temperature is very high so that this star is relatively bright. Nevertheless, both of these stars are far more compact than expected for a normal white dwarf. Indeed, in Ref. [24] it was concluded that an iron core might be required to provide the required compactness as illustrated on Figure 1.

On the other hand, other stars (e.g. *Sirius B*, *Procyon B*, and *40 Eri B*) fall nicely along the normal white-dwarf mass-radius relation. Hence, there is a hint of evidence for the existence of two white dwarf populations, one significantly more compact than the other.

A straightforward projection of the distribution of white-dwarf radii, however, obscures the two populations due to the fact that one is also dealing with a distribution of masses. To remove the mass effect from the distribution of radii, we wish to construct mass-radius relations which pass through each star. This is easily facilitated by the fact that the mass-radius relations for different compositions are nearly parallel for the range of masses of interest here (cf. Fig. 1). Thus, curves which pass through each star can be constructed from the parallel displacement of a single curve.

The implied distribution of radii corresponding to a fixed representative mass of 0.5 $M_\odot$ is shown on Figure 2. This plot is constructed from the sum of Gaussian distributions for each point with a width corresponding to the uncertainty in the radius of each star. With only 22 stars in the sample, the statistical and measurement errors are too marginal to conclude that there is unambiguous evidence for a bimodal distribution. Nevertheless, there is a hint of two peaks in this distribution. One is a rather narrow peak corresponding to the expected white dwarf radius around $R \approx 0.014 \pm 0.005\ R_\odot$ corresponding to normal white dwarfs. Below this peak there is a somewhat broader

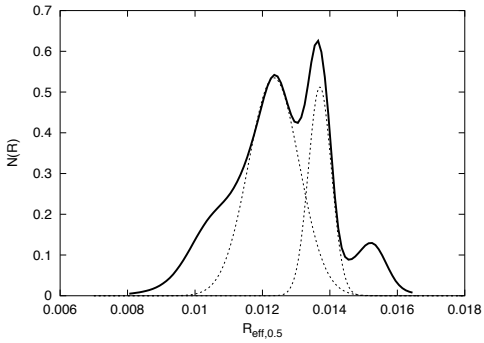

FIG. 2: Deduced distribution in radii for white dwarfs with a fixed effective $M = 0.5$ M$_\odot$. Dotted lines show gaussian fits to the two main peaks.

distribution centered at $R = 0.012 \pm 0.010\ R_\odot$. The total distribution is well fit with two gaussians as shown by the dotted lines on Figure 2.

The lower end of the radius distribution is comprised of the eight compact white dwarfs extending down to $R \sim 0.01$ $R_\odot$. These are identified on the bottom of Table 1. These compact stars may be members of a compact population. In addition, above the normal peak there are a few field stars with larger radii and large uncertainties. These presumably result from effects of the white-dwarf model atmosphere used in the determination of the field white dwarf radii [24, 38] and are probably not evidence for a population with large radii.

The more-compact component of the radius distribution is roughly what one might expect if a significant fraction of stars have accreted a strange-quark nugget during their main-sequence lifetime. Stars which have not developed a strange-matter core will be narrowly centered around the normal white dwarf radius. Those with strange-matter interiors would be expected to have cores which will have grown to their maximum size. The corresponding radius is $\sim 80\%$ that of normal white dwarfs [11] as we now show.

II. THE MODEL

To construct mass-radius relations we numerically integrate the Tolman - Oppenheimer - Volkoff (TOV) equation for general relativistic hydrostatic equilibrium.

$$\frac{dP}{dr} = -\left(\frac{GM_r}{r^2}\right)\frac{(\rho + (P/c^2))(1 + (4\pi P r^3/M_r c^2))}{(1 - (2GM_r/rc^2))} \quad . \tag{1}$$

with M_r the interior mass,

$$M_r = \int_0^r 4\pi r^2 \rho dr \quad , \tag{2}$$

and the pressure P is related to the matter mass density ρ through an appropriate equation of state (EOS).

For normal white dwarfs and normal matter in strange dwarfs we utilize the standard EOS of [13, 27]. This EOS produces the mass-radius relationships shown in Figure 1. For these curves, the central density, ρ_c varies from 10^5 to 10^{10} g cm^{-3}. As noted previously, a number of stars surveyed by *Hipparcos* have radii which are less than the radius expected for a C/O white dwarf.

III. MODIFICATIONS OF THE WD EOS

We have made a systematic study of all correction terms to the white dwarf equation of state, e.g. Coulomb correction, lattice energy, exchange energy, Thomas-Fermi correction, correlation energy, etc. We have even considered possible effects of magnetic fields [30]. None of these corrections can be reasonably varied to fit these compact white dwarfs for a normal He, C, or even Mg white dwarf.

A. Iron-core white dwarfs

As noted in [24], the only equation-of-state parameter which can be modified to account for these data is the composition. The main dependence is through the charge to baryon ratio Z/A which appears in the dominant noninteracting degenerate-electron term.

$$P_0 = \frac{mc^2}{24\pi^2}\left(\frac{mc}{\hbar}\right)^3 f(x) \quad , \tag{3}$$

where

$$f(x) = x(2x^2-3)(x^2+1)^{1/2} + 3\sinh^{-1} x \quad , \tag{4}$$

and

$$x = \left(\frac{\hbar}{m_e c}\right)\left(\frac{3\pi^2}{m_p}\frac{Z}{A}\rho\right)^{1/3} \quad . \tag{5}$$

In the nonrelativistic limit, the white dwarf radius roughly scales as $(Z/A)^{5/3}$. Decreasing Z/A from 0.5 to 0.46 appropriate to an iron composition sufficiently diminishes the radius so as to be consistent with the most compact stars in this sample.

Achieving such an iron-core white dwarf, however, is difficult from a stellar evolution standpoint. Single stars with $M \leq 8$ $M_\odot$ are thought to terminate their evolution with the formation of an electron-degenerate C/O core [14]. Stars with $M \approx 8$ to 11 $M_\odot$ probably collapse during nuclear statistical equilibrium burning without ever developing an iron core [39, 40]. The formation of an iron core only occurs during the final episode of quasi-equilibrium silicon burning at the end of the evolution of a massive ($M \geq 11$ $M_\odot$) progenitor star. The final episode of silicon burning to an iron core is exceedingly rapid both due to the high nuclear burning temperatures and the fact that the energy content per gram is diminished as the composition of the core shifts to heavier nuclei. The formation of the iron core in silicon burning typically lasts for only $\sim$ days and unavoidably proceeds until the core mass exceeds the Chandrasekhar mass. The end result is collapse to a proto-neutron star. Furthermore, even if one could somehow halt this rapid thermonuclear burn to the Chandrasekhar mass, it is difficult to imagine how to eject the outer layers of the star to expose the inner iron-core white dwarf.

B. Binary evolution

Another possibility might be some sort of exotic binary evolution. For example, Roche lobe overflow from one member of a binary can expose the white-dwarf core during a common envelope phase [15, 16]. However, this process typically requires at least 10^3 to 10^5 years and is unlikely to be completed just at the time at which the iron core is rapidly forming.

One could also imagine that a gradual mass deposition onto a white dwarf might somehow lead to episodic thermonuclear burning episodes which could produce an iron core. Effects of mass accretion onto a white dwarf have been studied for some time (cf. [17, 23, 39]). Most mass accretion rates ultimately lead to either a carbon detonation or deflagration type Ia supernova which leaves no white-dwarf remnant. There is a narrow region, however, for $M \sim 1.2$ $M_\odot$ and $\dot{M} \sim 10^{-9}$ in which helium detonates prior to carbon ignition so that no carbon detonation occurs. The resulting white-dwarf remnant, however, does not contain an iron core. There does not seem to be a middle ground. The conditions necessary to burn white-dwarf material to iron require such high densities and rapid reaction rates that it would seem impossible to fine tune the parameters of an accreting white dwarf to avoid the thermonuclear runaway associated with a Type-Ia supernova and disruption of the star.

IV. STRANGE-MATTER EOS

Strange matter, presents an alternative explanation for the existence of compact white dwarfs. Strange stars have smaller radii. This is simply because the density of strange quark matter is very high (> 2 times nuclear matter density). The density is so high for two reasons. One is that the QCD vacuum energy does not overwhelm the degeneracy pressure from the quarks and gluons until high density. Once the QCD vacuum energy dominates, one does not require gravity to maintain strange matter. Strange-quark matter is self bound and the star has no trouble to maintain the matter in hydrostatic equilibrium. Another factor contributing to the high density of strange-quark matter is the existence of three different quark fermion species within the core as opposed to only two in ordinary quark matter, or only one in the case of a simple electron-degenerate white dwarf. The additional degrees of freedom for strange-quark matter lower the degeneracy pressure and Fermi energy and allow the matter to be more compact.

A strange white dwarf is expected [9, 10] to consist of three distinct regions, a crust, a core-crust boundary, and a core. Each region requires a different EOS as we now describe.

A. Crust

The crust of the star is composed of normal degenerate matter. For the present purposes we take this crust to be predominantly composed of ^{12}C with a Hamada & Salpeter (1961) equation of state. Within the crust the density varies, but it is limited to be less than the neutron drip density, $\rho_{drip} = 4.3 \times 10^{11}$ g cm^{-3}.

B. Crust-core boundary

At densities higher than ρ_{drip} free neutrons are released from nuclei. These would gravitate to the core where they would be absorbed and converted into strange matter [9–11]. As long as this continues, the strange-matter core will grow. However, it is expected [1] that a sharp boundary between the inner core and the outer crust will develop at the point at which the crust density falls just below the neutron drip density.

This gap between the strange-matter core and the outer crust develops due to a Coulombic repulsion. Strange matter has a net positive charge because the finite ($\sim$ 150 MeV) mass of the strange quark prevents them from forming in sufficient quantities to maintain neutral strange matter. The degenerate electrons are unable to fully neutralize the positive charge of the inner strange-matter core because they are not bound by the strong interaction which keeps the core compact. Hence, a net positive charge exists in the strange-matter core. A dipole layer of very high voltage develops between the crust and the core.. This high voltage potential isolates the core from the outer crust which it also polarizes.

A slight gap thus exists between the core and crust regions. This prevents the further growth of the core beyond the radius associated with the neutron drip density. Hence, we take the radius at which the neutron-drip density is achieved as the inner boundary of the crust. This also defines the natural size to which the strange-quark core can grow.

C. Core

The core of the star is taken to be comprised of up, down and strange quarks. The *MIT* bag model equation of state is adequate for our purposes. The pressure is thus related to density by

$$P = (\rho - 4B)/3 \quad , \tag{6}$$

where ρ is the mass-energy density contribution dominated by noninteracting $\approx$ massless u and d quarks and gluons plus an s quark with $m \approx 150$ MeV. The quantity B is the bag constant which denotes the QCD vacuum energy. The bag constant is constrained from hadronic properties to be, $B^{1/4} \sim 145$ to 160 MeV. Within the quark core, the density is on the order of $2-3$ times nuclear matter density ($\sim 4-6 \times 10^{14}$ g cm^{-3}. The equation of state for strange dwarfs is illustrated in Figure 3. This shows the transition to strange quark matter which takes place at the neutron drip density. Although the density steps discontinuously, the star remains in pressure equilibrium and the pressure varies continuously through the star.

Having specified the EOS, we have radially integrated the TOV equation for various initial central densities until the density falls below a minimum density of $10^{-9} \times \rho_{drip}$. Examples of the interior radial profiles of both a normal and a strange-matter white dwarf are shown in Figure 4. Here, one can see that most of the outer crust looks quite

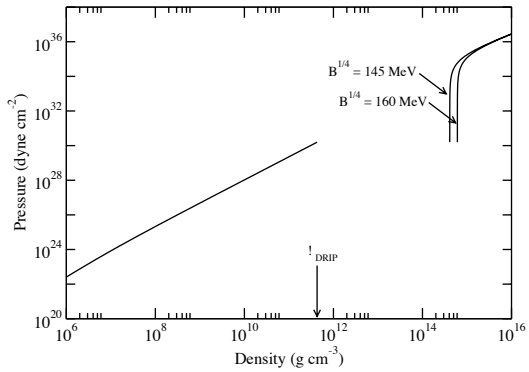

FIG. 3: Illustration of the strange-matter equation of state.

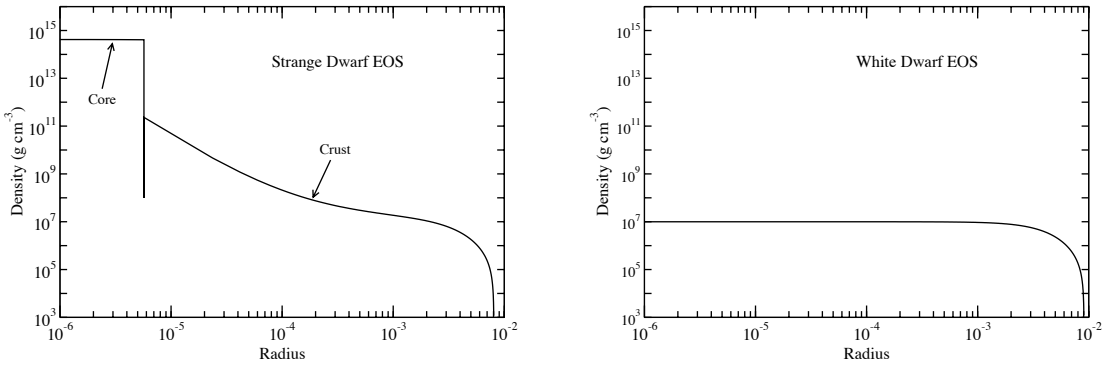

FIG. 4: Illustrations of the interior density vs. radius for a strange-matter white dwarf (upper figure) and a normal-matter white dwarf (lower figure). The separation between the core and crust regions is indicated in the upper curve.

similar to a normal white dwarf. A deviation from the normal white dwarf density profile is only apparent for the inner few percent of the radius of the star. Nevertheless, the existence of the compact inner core leads to a smaller surface radius for the strange dwarf.

For models with $B^{1/4} = 145$ MeV, the central density ρ_c varies from 4.1 - 4.2 $\times$ 10^{14} g cm^{-3}. In models with $B^{1/4} = 160$ MeV, ρ_c varies from 6.1 - 6.2 $\times$ 10^{14} g cm^{-3}. At these densities, strange dwarfs are in a mass range comparable to that for ordinary white dwarfs, i.e. $0.3M_\odot \leq M \leq 1.35M_\odot$. In [9, 10] a radial pulsation analysis is performed which demonstrates that these strange dwarfs are indeed stable.

D. Color Superconductivity

Here a few remarks about the possible existence of color superconductivity in strange-quark matter are warranted. It is now generally accepted [2, 26] that quark matter at high density may be in a so-called color-flavor locked (CFL) state, with equal numbers of u, d, and s quarks. This CFL state could be the ground state of strong interaction and therefore stable even though the quark masses are unequal. On the other hand, quark matter at the "lower" densities of interest here [34] may be a 2-flavor superconductor, 2SC, rather than a CFL superconductor. The 2SC state is characterized by a much smaller pairing gap and very similar to the simple bag model equation of state (Eq. 6) employed here.

Moreover, even for CFL strange-matter, the thermodynamic potential is given as $\Omega_{CFL} = \Omega_{free} - B_{eff}$, where Ω_{free} is the thermodynamic potential for ordinary unpaired quarks and $B_{eff} = -3\Delta^2\mu^2/\pi^2 + B$ [20], where Δ is the gap of the QCD Cooper pairs, μ is the average quark chemical potential, and B is the bag constant of Eq. (6). In this

case, B_{eff} is actually not constant but depends upon the chemical potential μ. However, by adopting a characteristic mean value of the chemical potential for CFL strange matter, we can set B_{eff} as an overall constant. With this simplification, if we can use this B_{eff} instead of B in the Eq. (6), the only effect is an overall shift of structural properties by some constant. Even for large gaps, the equation of state (Eq. 6) is only modified by a few percent of the bulk energy. Such small effects can be safely neglected in the discussions here. Therefore, the equation of state of Eq. (6) remains adequate for our purpose by simply exchanging B_{eff} for B.

Another issue associated with a CFL strange-matter core in the configuration of strange dwarfs is halting the growth of the charge neutral CFL strange-matter core. In Ref. [26] it has been shown that the CFL phase is electrically neutral in bulk without any need for electrons. However, as mentioned in Sec. IV B, in order to prevent the further growth of the core, the strange-matter core should have a net positive charge. This produces a gap of very high voltage between the strange-matter core and the outer crust due to Coulombic repulsion around the neutron drip density. The CFL strange-matter consists of equal numbers of u, d, and s quarks and is electrically neutral. In the absence of electrons it seems difficult to build a gap of high voltage between the CFL strange-matter core and the outer crust. However, if these stars are in the 2SC phase, they do contain electrons so that the formation of an electric dipole layer at the surface of a superconducting 2SC strange quark matter core is not a problem at all.

Moreover, in Ref. [31] it has been shown that thin layers at the surface of CFL strange-matter are no longer electrically neutral as in the bulk because of surface effects [21]. That is, in the surface of CFL strange-matter the number of massive quarks is suppressed relative to the number of massless quarks at fixed Fermi momentum. This leads to a net increase in the total electrical charge at the surface of CFL strange-matter. Therefore, we will assume that the Coulombic repulsion mechanism for the halting of strange-matter core growth remains valid even for CFL or 2SC strange dwarfs.

V. RESULTS AND DISCUSSION

The mass-radius relation for strange-matter white dwarfs is shown in Figure 5 and compared with that derived from the normal-matter white-dwarf equation of state with various composition. The curves for strange dwarfs agree surprisingly well with several of the best determined data points. Of greatest importance are *G238-44*, *EG 50* and *GD 140*. As mentioned earlier, these stars have well determined masses, and they lie very close to the strange dwarf mass radius relation. As a quantitative measure of the improvement to the fit to the distribution. We have evaluated the effects on the total χ^2 by associating each star with one curve or the other. The stars which minimize χ^2 by association with the strange-dwarf mass-radius relation are identified as candidates in Table 1. The total χ^2 if all stars are associated with a normal carbon white-dwarf EOS is 119 corresponding to a reduced $\chi^2_r = 5.2$ for 23 degrees of freedom. If we allow an iron-core population with members chosen to minimize χ^2 we have is 105 ($\chi^2_r = 4.4$ with 24 degrees of freedom). This is to be compared with a value of 78 ($\chi^2_r = 3.2$) when eight stars are identified with a strange-matter EOS instead. Hence, even allowing for the fact that an extra degree of freedom has been introduced by assigning membership in one population or the other, we have a $\Delta\chi^2 = 41$ ($\sim 6\sigma$) preference for the presence of a strange-dwarf population over a normal EOS versus only a $\Delta\chi^2 = 14$ ($\sim 4\sigma$) improvement with an iron-core population.

A. Observational tests

Having identified these candidate stars as possible strange dwarfs one would like to speculate on other observations which might be used to discriminate between a normal white dwarf and a strange star. There are two possibilities which immediately come to mind. Both of them are based upon astroseismology. One could be the filtering of those pulsation modes which are most sensitive to the transition region between normal and strange matter. The other might be the effects of strange-dwarf cooling rates on the observed pulsations.

Regarding astroseismology, nonradial g-mode pulsations of white dwarfs are observed to occur in three different phases of their evolution (cf. [6]). At temperatures above 80,000 K some hydrogen-deficient DOV white dwarfs and some planetary nebulae are observed to pulsate. Also at cooler temperatures $T_{eff} \approx 16,000$ to 25000 K [36, 37], some helium dominated DBV stars are observed to pulsate. Since almost all of the stars in the present sample are DA white dwarfs with hydrogen-dominated spectra, it is particularly noteworthy that a narrow strip exists [4, 12] for $T_{eff} \approx 12,000$ K in which DAV (or *ZZ Ceti*) stars are observed to pulsate. Unfortunately, however, only one star (*G*226-29) in this sample falls within the DAV pulsation strip and this star is not a candidate for a strange matter core. The pulsations of this star have been reanalyzed [19] using the *HST*. Its inferred mass and radius are consistent with a normal white dwarf and there is nothing peculiar in the pulsation spectrum. On the other hand, we point out

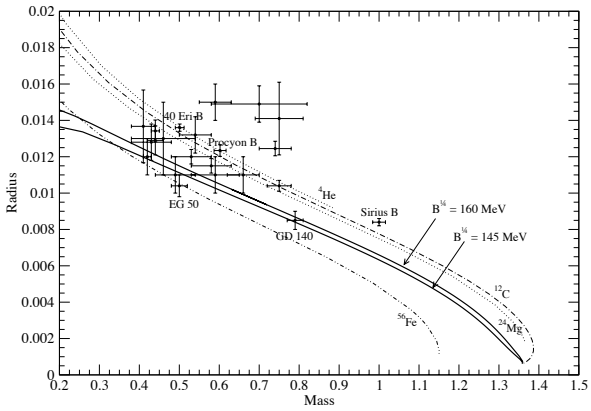

FIG. 5: Comparison of the theoretical mass-radius relationships for strange dwarfs (solid curves) and normal white dwarfs with the data of [24, 25].

that two of the strange-dwarf candidates, *G181-B5B* and *GD 279* are tantalizingly close (within uncertainty) to the DAV instability temperature and may perhaps warrant further study to search for peculiar pulsations.

If a pulsating strange-dwarf candidate were ever to be found, one would expect its properties to be similar to a normal DAV with some slight changes. It would be similar because the bulk of the volume of the star is still dominated by a normal matter crust as evident in Figure 4. On the other hand the development of a steep abundance gradient in the normal matter for the inner $\approx$1% of the star followed by the sharp discontinuity at the strange-matter core could have some observational consequences. One might propose a test along the following lines.

For idealized g-modes, the pulsations are approximately evenly spaced with periods given by [18],

$$\Pi_{nl} = \frac{\Pi_0}{\sqrt{l(l+1)}}(n+\epsilon) \quad , \tag{7}$$

with Π_0 a constant determined by the internal structure.

$$\Pi_0 = (2\pi)^2 \left[\int \frac{N}{r} dr \right]^{-1} \quad , \tag{8}$$

where N is the Brunt Väisälä (buoyancy) frequency. The simplest effect for a more compact star then is that the radial integral in Equation (8) changes. On the one hand, the integral extends over a smaller radius, while the larger densities would imply a larger buoyancy frequency. Anticipating that the latter effect is dominant, one would expect shorter period oscillations for the more compact dwarfs.

Equation (7), however, only holds for stars with homogeneous composition. The steep density gradient as one approaches the strange-matter core will produce a rapid change in the buoyancy frequency. This will lead to mode trapping. That is, modes that have nodes in the region where the density is changing rapidly will have the amplitude of their eigenfunctions significantly reduced. This small amplitude in the interior implies that less energy is required to excite and maintain such modes. The kinetic energy of a nonradial mode can be written [18]:

$$E_K \propto \frac{\sigma^2}{s} \int_o^R \rho r^2 dr \left[\xi_r^2 + l(l+1)\xi_h^2 \right] \quad , \tag{9}$$

where ξ_r and ξ_h refer to the perturbation displacement in the radial and horizontal directions, respectively. The presence of the density ρ in the integral, however, implies that small oscillations within the high-density core can contribute significantly to the kinetic energy.

Thus, the smallest kinetic energies will be associated with trapped nodes which have diminished interior amplitudes, but also with lower modes with less displacement in the high-density core. This is important since the growth rate for the amplitude of the mode scales as $1/E_K$. Hence, these particular trapped modes will be the most easily excited in the spectrum. Indeed, this filtering effect which enhances the excitation of specific modes is well understood [35]

in normal DAV white dwarfs where this effect arises from the hydrogen/helium discontinuity. Here we speculate that a similar and perhaps more dramatic effect may occur from the crust-strange-matter discontinuity.

Following this line or reasoning, we suggest that the periods of the trapped modes in the outer layers of the star should obey,

$$\Pi_i^2 = 4\pi^2\lambda_i^2\left[\left(1-\frac{r_{core}}{R}\right)l(l+1)\frac{GM}{R^3}\right]^{-1} \quad , \tag{10}$$

where λ_i are constants relating to the zeros of Bessel functions and the index i corresponds to the number of nodes between the surface and the core transition region which occurs at a radius r_{core}. We propose therefore, that in principle one could use the identification of these trapped modes to find the radius and mass of the inner transition to a strange-matter core.

Regarding cooling rate, it is generally appreciated that strange neutron stars would cool more rapidly than normal neutron stars due to the loss of interior energy by neutrinos produced from the weak decays to strange matter [1]. We speculate that a similar process may be in operation early in the life of a hot strange dwarf. In such stars, the core may still be growing to its putative equilibrium size and might be identified as a hot pulsating star with an anomalously large cooling rate. If the core is in the CFL phase, it has a superfluid gap that may be as large as ~ 100 MeV. Such large gaps render the quark matter core almost thermally "inert" since the heat capacity and neutrino emissivity are proportional to exp(-kT/Delta). The cooling behavior of strange dwarfs with crusts would thus almost entirely be determined by the strange dwarf's nuclear crust and they would appear cool very quickly. On the other hand, if the core is in the 2SC phase, which has a much smaller gap ($\sim$ keV's to MeV's), the rapidly cooling quark matter core should have a significant impact on the apparent thermal evolution. Either way, the stars would appear to have an anomalously rapid cooling rate.

Indeed, cooling rates have been observed [36, 37] in hot DOV stars as they evolve from planetary nebulae to the white-dwarf cooling phase. Such stars are evolving so rapidly that one can measure changes in the pulsation periods which relate directly to the cooling rate of the star. We thus propose that the identification of a compact DOV white dwarf with an anomalously high cooling rate may constitute an independent confirmation of the development of a strange-matter core.

An opposite effect, however, is possible if a strange dwarf is a member of an accreting binary. The strange dwarf would respond to the accretion of matter by converting some of the material in the crust to strange matter. The released latent heat would raise the interior temperature and therefore require a longer timescale to radiate away energy than that of a normal-matter white dwarf.

VI. CONCLUSIONS

The purpose of the present study has been to explore the possible existence of a new population of compact white dwarfs and whether such compact stars are consistent with an interpretation that they contain strange-matter cores. At present the data are too sparse and uncertain to conclusively determine whether or not any of this sample of DA white dwarfs are strange dwarfs. Nevertheless, we have shown that the deduced masses and radii are at least marginally consistent with an interpretation that some stars in the sample contain strange-matter cores. Although this seems exotic, we have argued that the alternative interpretation of iron-core white dwarfs is difficult to achieve from a stellar evolution standpoint and does not fit the observed compact population as well with a single curve.

Clearly, more data on the masses and radii for white dwarfs would be of immense help in determining whether there exists a population of compact white dwarfs. Of particular interest would be the discovery of a strange-dwarf candidate in the DAV (or DOV) pulsation mode. One might be able to detect the presence (or formation) of a high density strange-matter core from the associated mode filtering.

Acknowledgments

The author's wish to acknowledge useful input from Tom Guthrie and Doran Race in various aspects of the data analysis. Work supported in part by the US Department of Energy under Nuclear Theory grant DE-FG02-95ER40934. Work of B.O. supported in part from the National Science Foundation a Research Experience for Uundergraguates grant at the University of Notre Dame. One of the authors (KO) wishes to acknowledge support from the Japanese Society for the Promotion of Science and by NSF grant PHY 02-16783 for the Joint Institute for Nuclear Astrophysics (JINA). The research of F. W. is supported in part by the National Science Foundation under Grant PHY-0457329,

and by the Research Corporation.

---

[1] Alcock, C., Farhi, E. & Olinto, A. 1986, ApJ, 310, 261
[2] Alford, M., Rajagopal, K., Wilczek, F. 1999 Nuc. Phys. B, 537, 433
[3] Bagchi, M., Ray, S., Dey, M. & Dey, J. 2006, MNRAS in press, astro-ph/0602348
[4] Bergeron, P. et al. 1995, ApJ, 449, 258
[5] Bergeron, P., Leggett, S. K. & Ruiz, M. T. 2001, ApJS, 133, 413
[6] Brown, T. M. & Gilliland, R. L. 1994, ARA&A, 32, 37
[7] Drake, J. J. et al. 2002, ApJ, 572, 996
[8] Fontaine, G. et al. 2001, ApJ, 557, 792
[9] Glendenning, N. K., Kettner, Ch. & Weber, F. 1995a, Phys. Rev. Lett., 74, 3519
[10] Glendenning, N. K., Kettner, Ch. & Weber, F. 1995b, ApJ, 450, 253
[11] Glendenning, N. K. & Weber, F. 1992, ApJ, 400, 647
[12] Greenstein, J. 1982, ApJ, 258, 661
[13] Hamada, T. & Salpeter, E. E. 1961, Astrophys. J. 134, 683
[14] Iben, I. Jr. & Renzini, A. 1983, ARA&A, 21 271
[15] Iben, I. Jr. & Tutukov, A. V. 1984, ApJS, 54, 355
[16] Iben, I. Jr. & Tutukov, A. V. 1985, ApJS, 58, 661
[17] Iwamoto, K. et al. 1999, ApJS, 125, 439
[18] Kawaler, S. D. & Bradley, P. A. 1994, ApJ, 427, 415
[19] Kepler, S. O. et al. 2000, ApJ, 539, 379
[20] Lugones, G & Horvath, J. E., 2003, A&A, 403, 173
[21] Madsen, J. 2001, Phys. Rev. Lett. 87, 172003
[22] Majczyna, A. & Madej, J. 2005, Acta Astron., 55, 1
[23] Nomoto, K., Thielemann, F.-K., and Miyaji, S. 1985, A&A, 149, 239
[24] Provencal, J. L., Shipman, H. L., Hog, E., & Thejll, P. 1998, Astrophys. J. 494, 759
[25] Provencal, J. L. et al. 2002, Astrophys. J. 568, 324
[26] Rajagopal, K., & Wilczek, F., 2001, Phys. Rev. Lett. 86, 3492
[27] Salpeter, E. E. 1961, Astrophys. J. 134, 669
[28] Schaffner-Bielich, J. 2005, J. Phys. G31, S651
[29] Slane, P. O., Helfand, D. J., & Murray, S. S. 2002, ApJL, R571, L4
[30] Suh, I.-S. & Mathews, G.J. 2000, ApJ, 530 949
[31] Usov, V. V. 2004 Phys. Rev. D 70, 067301
[32] van Leeuwen, F. 2005, Astron. & Astrophys., 439, 805
[33] Vartanyan, Yu L., Grigoryan, A. K. & Sargsyan, T. R. 2004, Astrophysics, 47, 2004 (189)
[34] Weber, F. 2005, Prog. Particle & Nucl. Phys., 54, 193
[35] Winget, D. E., Van Horn, H.M. & Hansen, C. J. 1981, ApJL, 245, L33
[36] Winget, D. E., Hansen, C. J. & Van Horn, H. M. 1983, Nature, 303, 781
[37] Winget, D. E., et al. 1983, ApJL, 268, L33
[38] Wood, M. A. 1990, Ph.D. thesis, Univ. of Texas at Austin
[39] Woosley, S. E. & Weaver, T. A. 1986, ARA&A, 24, 205
[40] Woosley, S. E. & Weaver, T. A. 1995, ApJS, 101, 181
[41] Xu, R. X., 2005, MNRAS, 356, 359

TABLE I: Adopted[a] White Dwarf Properties

Star	$M/M_\odot$	$R/R_\odot$	$T(K)$
Normal White Dwarfs			
Sirius B	1.0034 ± 0.026	0.00840 ± 0.00025	24700 ± 300
G226-29	0.750 ± 0.030	0.01040 ± 0.0003	12000 ± 300
G93-48	0.750 ± 0.060	0.01410 ± 0.0020	18300 ± 300
CD -38 10980	0.740 ± 0.040	0.01245 ± 0.0004	24000 ± 200
L268-92	0.700 ± 0.120	0.01490 ± 0.0010	11800 ± 1000
Stein 2051B	0.660 ± 0.040	0.0110 ± 0.0010	7100 ± 50
Procyon B	0.602 ± 0.015	0.01234 ± 0.00032	7740 ± 50
Wolf 485 A	0.590 ± 0.040	0.01500 ± 0.0010	14100 ± 400
L711-10	0.540 ± 0.040	0.01320 ± 0.0010	19900 ± 400
L481-60	0.530 ± 0.050	0.01200 ± 0.0040	11300 ± 300
40 Eri B	0.501 ± 0.011	0.01360 ± 0.0002	16700 ± 300
G154-B5B	0.460 ± 0.080	0.01300 ± 0.0020	14000 ± 400
Wolf 1346	0.440 ± 0.010	0.01342 ± 0.0006	20000 ± 300
Feige 22	0.410 ± 0.030	0.01367 ± 0.0020	19100 ± 400
Candidate Compact Strange Dwarfs			
GD 140	0.790 ± 0.020	0.00854 ± 0.0005	21700 ± 300
G156-64	0.590 ± 0.060	0.01100 ± 0.0010	7160 ± 200
EG 21	0.580 ± 0.050	0.01150 ± 0.0004	16200 ± 300
EG 50	0.500 ± 0.020	0.01040 ± 0.0006	21000 ± 300
G181-B5B	0.500 ± 0.050	0.01100 ± 0.0010	13600 ± 500
GD 279	0.440 ± 0.020	0.01290 ± 0.0008	13500 ± 200
WD2007-303	0.440 ± 0.050	0.01280 ± 0.0010	15200 ± 700
G238-44	0.420 ± 0.010	0.01200 ± 0.0010	20200 ± 400

[a]Data from Provencal et al. (1998; 2002).